Kinking Nonlinear Elastic Solids, Nanoindentations, and Geology

M.W. Barsoum, A. Murugaiah, S.R. Kalidindi, and T. Zhen
Department of Materials Science and Engineering, Drexel University, Philadelphia, Pennsylvania 19104, USA
(Received 8 January 2004; published 25 June 2004)

The physical mechanism responsible for nonlinear elastic, hysteretic, and discrete memory response of nonlinear mesoscopic elastic solids has to date not been identified. We show, by nanoindenting mica single crystals, that this response is most likely due to the formation of dissipative and fully reversible, dislocation-based kink bands. We further claim that solids with *high c/a ratios*, which per force are plastically anisotropic, should deform by kinking, provided they do not twin. These kinking nonlinear elastic solids include layered ternary carbides, nitrides, oxides, and semiconductors, graphite, and the layered phases, such as mica, present in nonlinear mesoscopic elastic solids.

DOI: 10.1103/PhysRevLett.92.255508 PACS numbers: 81.05.–t, 62.20.–x

Many materials near the Earth's surface are believed to be nonlinear mesoscopic elastic (NME) solids that exhibit nonlinear elastic behavior, hysteresis, and discrete memory [1–3]. Currently, these solids are modeled phenomenologically by invoking the presence of hysteretic mesoscopic units (HMUs), whose physical underpinnings are unknown [1]. On the other hand, it has long been established that kink bands (KBs) play a role in the deformation of some geologic materials [4–7]. Herein we make the case that HMUs are nothing but incipient kink bands (IKB).

An incipient kink band is a thin sliver of material bounded by two, near parallel, dislocation walls of opposite polarity that attract each other [8–11] [inset (i) of Fig. 1(b)]. IKBs are fully reversible; the walls are kept apart by the applied stress σ and annihilate fully when it is removed [8–10]. The remote shear stress τ_k needed to render a subcritical kink band critical is given by [11,12]

$$\tau_k = \sqrt{\frac{2G^2 b\gamma}{\alpha}}, \tag{1}$$

where G and b are, respectively, the shear modulus and Burgers vector. α is the domain size available for the creation of the IKB and γ is the shear or kinking angle subtended by the subcritical kink band. When γ reaches a critical value of $\approx 3°–6°$, the subcritical KB becomes unstable and forms an incipient kink band [11]. For virgin layered polycrystalline solids α is nothing but the width of a grain measured normal to its basal planes, i.e., along the c axis [8]. Equation (1) is *fundamental* because it leads to the *key* domain-size-dependent hysteretic element of the Preisach-Mayergoyz (PM) space model [1,2]. At $\tau > \tau_k$ an IKB is triggered; conversely, upon unloading, and because of friction, the IKB is annihilated only when $\tau < \tau_0$ [inset (ii) of Fig. 1(b)]. The energy dissipated is due to the back and forth motion of the dislocations comprising the IKBs.

Experimentally, IKBs manifest themselves as fully *reversible* stress-strain hysteresis loops [8–10]. Since the dislocations are restricted to move on the basal planes, they cannot entangle, i.e., work harden in the classic sense, and the energy dissipated per cycle, W_d, can be quite high. Log-log plots of W_d versus applied stress σ result in straight lines with slopes of ≈ 2 [8–10]. At high enough temperatures [8] or stresses [9,10], the IKB walls separate and move away from the center of what eventually becomes the KB. The IKB to KB transformation results in the formation of microdomains that, per force, are smaller than the initial domain size. According to Eq. (1), this reduction in α leads to hardening [8–10].

That KBs play an important role in the deformation of plastically anisotropic solids, such as Ti_3SiC_2 [8,9], and graphite [10] is now established. In graphite the bonds between the planes are van der Waals; in Ti_3SiC_2 they are a combination of metallic, ionic, and covalent. This begged the question of whether KBs also play a role in ionically bonded solids such as mica. Herein we present nanoindentation evidence for the formation of IKBs and KBs in mica, and by extension other layered minerals. We also briefly discuss the far-reaching implications of these results for geology.

We examined natural muscovite single crystals commercially available (Hi-grade mica, grade V2, Ted Pella Inc., California, USA). The provenance and a detailed chemical analysis were not determined and are not necessary for the purpose of this study. The inset of Fig. 1(a) plots typical load/depth-of-penetration curves obtained when a diamond spherical nanoindenter (13.5 μm radius) is loaded to 100 mN normal to the basal planes. Successive indentations in the *same* location generated a series of hysteresis loops in which the first loop was slightly open, but subsequent loops were perfectly superimposable [Fig. 1(a)]. To account for the residual deformation present after the first indent, the second and subsequent load displacement curves were shifted such that their maximum displacements were identical to those of the first indents [Fig. 1(a)]. The small ≈ 12 nm gaps present upon total unloading of the second and subsequent loops [Fig. 1(a)] are an artifact of the experiment

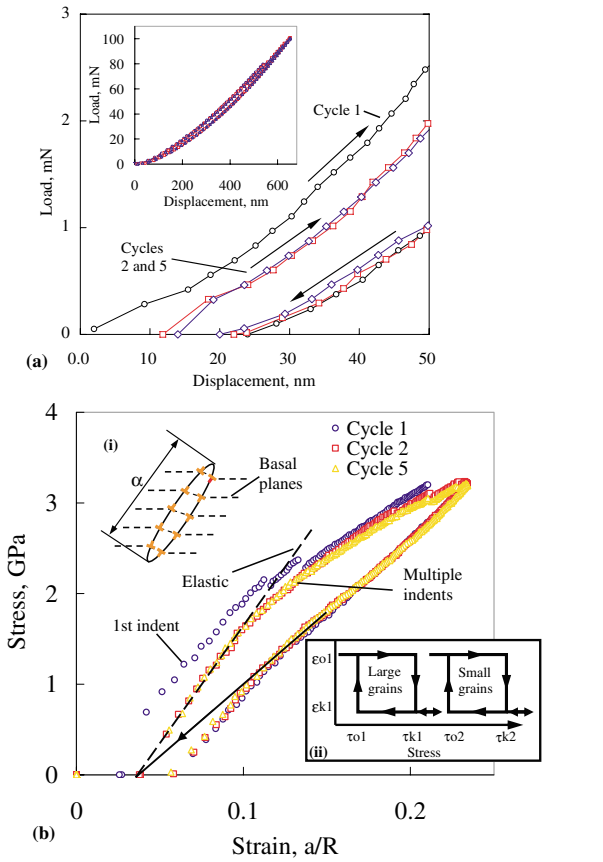

FIG. 1 (color online). (a) Typical load versus depth-of-indentation curves obtained by loading several times in the same location. The inset shows full scale of same results. (b) Stress/strain curves for data shown in (a). In both cases only cycles 1, 2, and 5 are shown. Inset (i) is a schematic of an IKB (see text). Inset (ii) is a schematic of how a microstructurally dependent, IKB-based, hysteretic element would behave on loading and unloading.

setup because (i) they were observed in silica that was loaded elastically and (ii) the excellent reproducibility of the load versus depth-of-penetration loops after the first cycle [Fig. 1(a)]. Note the areas encompassed by the loops decrease after the first indent, which is clear evidence for cyclic hardening.

The load/displacement curves were converted to stress/strain curves [Fig. 1(b)] [13,14](for details see Ref. [9]). The stress is the normal Hertzian contact stress, and the strain is the ratio of the contact area radius a to the indenter radius R. Here again the first loop is open, and second and subsequent loops are marginally so [Fig. 1(b)]. The deviation of the curves, at the end of unloading cycles, from the solid straight line drawn in Fig. 1(b) is an artifact of the experiment. In other words, the unloading curves should follow the straight line ending at the point at which the reloading cycles start. In general, the slopes of the first loading stress/strain curves were less steep than subsequent ones, plotted as a dotted straight line in Fig. 1(b). The slope of the dashed line corresponds to a c_{33} of 61 GPa; the latter was obtained from *ab initio* calculations [15].

A small but clear pop-in is observed at ≈ 2.2 GPa during the first loading in Fig. 1(b). This yield point is a strong function of the type and grade of mica used. Lower grade micas, with presumably larger numbers of defects, tended to have lower yield points. Higher-grade micas behaved elastically up to quite high stresses, of the order of 7 GPa.

Simple compression tests were carried out on mica-containing glass-ceramic cylinders (12.7 mm in diameter, 31 mm long). The stress/strain curves [16] exhibited fully closed hysteresis loops (not shown) that were quite similar to those obtained in graphite [10].

Figure 2 is a log-log plot of W_d vs σ obtained in this work together with the corresponding values for Ti_3SiC_2 and graphite, obtained from bulk [8] and nanoindentation experiments [9,10] similar to the ones shown here (Fig. 2).

Our kink-band-based model can readily explain the full reversibility of the process, the cyclic hardening, and the large values of W_d. The reversibility is inherent to the IKBs since, by definition, they are fully reversible [8–10]. The confinement of dislocations to the basal planes [17–19] allows the dislocation loops to extend over relatively large distances resulting in large values of W_d (Fig. 2). Note that the glide of dislocations *per se* cannot explain this phenomenon since glide is irreversible.

The large values of W_d imply that the areas swept by the dislocation lines must be huge, a conclusion reached by both Meike [17] and Kronenberg *et al.* [18]. The former directly observed basal dislocation motion in the TEM and reported dislocation separations, attributed to stacking faults, of the order of 100 to 500 nm. In the same paper, Meike showed dislocation segments in mica of the order of 20 μm. Kronenberg *et al.* [18] working with

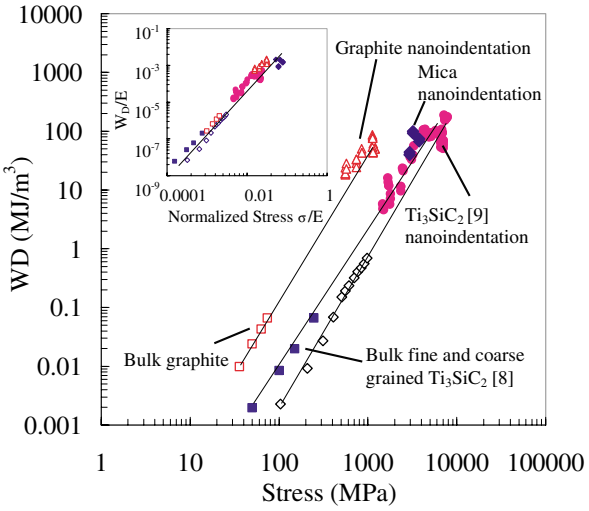

FIG. 2 (color online). Log-log plot of W_d vs σ_{max} for mica, Ti_3SiC_2, and graphite. The inset shows the same plot with axes normalized by either Young's moduli (bulk) or c_{33}. For mica, c_{33} is 61 GPa [15].

biotite single crystals concluded that the activation areas were "enormous" and were irreconcilable with the dearth of stacking faults found in TEM foils of deformed samples.

At higher stresses, the IKBs are sundered and devolve into parallel *mobile* dislocation walls. It is the coalescence of these walls into kink boundaries that eventually gives rise to kink bands [20–22], and simultaneously lead to the cyclic hardening observed. Given that hardening has to be dislocation based and kinking is known to occur in mica [4–7,17–19], it is reasonable to conclude that our kinking based model, used successfully to explain similar behavior in Ti_3SiC_2 [8,9] and graphite [10], is also applicable here. The most compelling evidence, however, that the *same* mechanisms are operative in all three compounds, is the universal curve obtained (inset of Fig. 2) when both axes in Fig. 2 are normalized by the appropriate elastic stiffnesses (Young's moduli for the bulk samples and c_{33} for the nanoindentation results).

Indentations to loads higher than 400 mN resulted in massive, very sudden, and irreversible penetrations of the order of 2 μm (not shown). Subsequent indentations in the same location once again resulted in loops that became harder and closed with cycling. In the absence of such massive pop-ins, and despite the fact that the Hertzian stresses at the tip of the indenter were of the order of 4 GPa for the higher loads, typically *no trace* of the indentations was found in the field emission scanning electron microscope (FESEM).

Typical FESEM micrographs of postindentation craters formed after massive penetrations of the indenter are shown in Fig. 3. The indenter clearly left an indent with some cracks emanating from its center [inset of Fig. 3(a)]. The sharp bends, denoted by arrows [Fig. 3(b)] and their orientation relative to the basal planes, have to be kink boundaries. The massive rotation of the lattice planes is unambiguous. At higher magnifications the pileups around the indenter are revealed to be delaminated basal planes [inset of Fig. 3(b)]. Note the fine scale of the delaminations. Such features are ubiquitous in Ti_3SiC_2 and have been observed at all lengths scales [20–26]. Figure 3(a) also provides irrefutable direct evidence for the breakup of the single crystal into smaller grains, a key assumption in our model. Almost identical microdomains were observed in indented graphite single crystals [10].

Delaminations are inherent to the IKB to KB transformation because an IKB cannot dissociate without delamination. Such delaminations at tips of dislocation walls subjected to shear stresses were predicted by Stroh [27]. The delaminations most probably occur at the intersection of dislocation walls and arrays, eliminating the latter [21]. Note that the dislocation arrays are also inherent to the overall process; without them, the various lamellae could not shear relative to each other, the precursor for all that follows [20,21]. Such arrays have been observed in mica [28].

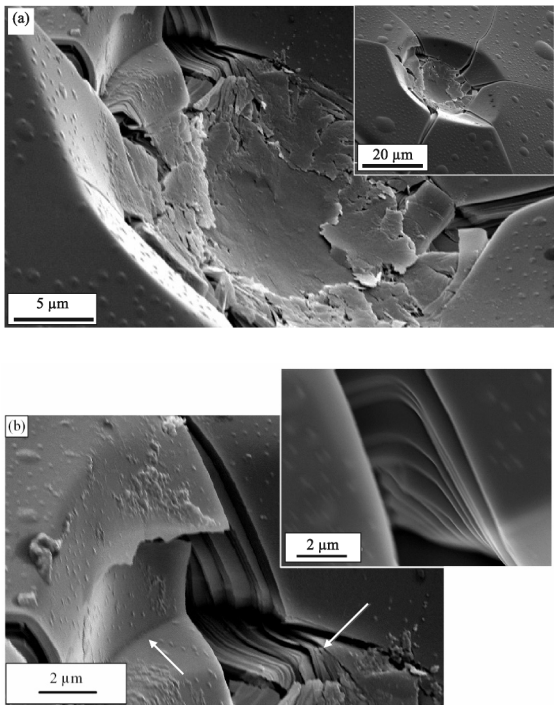

FIG. 3. FESEM micrographs of indents in mica after massive penetration. (a) Breakup of the pristine sheets of mica into a multitude of smaller domains (inset shows low magnification micrograph of the indent and characteristic pileup around indentation), and (b) higher magnification showing kinks denoted by arrows (inset shows typical delaminations).

At first glance any relationship between nanoindentations and geology may seem far fetched. However, since the deformation under an indenter, like that of many rocks, is constrained it is possible to reach much higher stresses, and thus better mimic geologic conditions, than would normally be possible. Futhermore, the relationship between σ and W_d allows for extrapolations to even higher stresses with some confidence (Fig. 2). Note that W_d cannot increase indefinitely—an upper limit must exist when α is of atomic dimensions—further enhancing our predictive capabilities.

The relevance of the results presented herein to geology cannot be overemphasized. First and foremost, the identification of the origin of the HMUs, viz. the formation of IKBs, operative in NME solids, should rapidly lead to a much deeper understanding, including the development of the requisite constitutive equations of this important class of solids. Needless to add, our model is consistent with all HMU-based models for which there has been a flurry of activity lately [1,2,29–31]. For example, based on this insight the response of NME solids can now be directly related to the volume fraction of the KB-prone phase. Such understanding is crucial, for example, in predicting the "site response" in earthquake engineering, which in turn has a major influence on designing structures for minimal damage due to earthquakes [1].

There are other important ramifications. First, since α is proportional to $1/\sigma^2$ and W_d at high stresses appears to

be a unique function of σ (Fig. 2), measurements of α could lead to an estimation of the maximal geostresses experienced by a KB-containing geologic formation. Second, the mechanical response of a geologic formation comprised of a layered mineral becomes not only a function of its composition, but also its thermomechanical history: the more a rock is deformed the more it hardens. Third, the elastic properties of any layered rocks that deform by KBs measured by ultrasound, which is how much of the information is obtained in the first place, are of dubious utility in predicting their macroscopic response. This is especially true since ultrasound in general does *not* initiate IKBs. Along the same lines, a solid under stress with a high density of KBs will have innumerable dislocation loops that, in turn, will respond to a perturbation, such as ultrasound, quite differently than the same rock with a different density of KBs. Fourth, the presence of KBs and the nonlinear nature of the deformation can significantly alter the amount of strain energy stored in a rock as compared to a purely elastic deformation, with obvious implications for seismology.

Based on this and previous [8–10] work it is evident that mechanically anisotropic solids, where a high c/a ratio is a sufficient *but not a necessary condition*, will deform by kinking, provided they do not twin. Thus a good descriptor of these solids is kinking nonlinear elastic (KNE) solids. KNE solids include layered minerals and ceramics, the layered phases in NME solids such as mica [1,2], the $M_{n+1}AX_n$ phases, where M is an early transition metal such as titanium, A is an A group element such as silicon, X is either carbon or nitrogen, and n varies from 1 to 3 [8,9,23], graphite [10], hexagonal boron nitride [16], and, most probably, ice [32], among many others. Given the diversity and ubiquity of these materials it is clear that IKBs and KBs play a much more important role in our daily life than has hitherto been appreciated. Furthermore, the fact these solids, in all their diversity and ubiquity, are subject to the same physics—two dislocation walls attracted to each other, with dislocations confined to basal slip and complications arising from strain hardening and twinning absent—is sublime.

In conclusion, the availability of a relatively simple nondestructive technique, which requires tiny samples to probe such solids at geologically relevant stresses, is a huge advantage that should lead to rapid advancement in our understanding and one that should prove of immense benefit. That nanoindentations that can tell us anything about how an earthquake will shake the Earth—a 15 orders of magnitude span of lengths scales—is remarkable.

We thank Dr. P. Finkel of Thompson Inc., PA, for pointing out Ref. [1] and its possible relevance to our work. This work was funded by ARO Grant No. DAAD19-03-1-0213 and the National Science Foundation Grant No. DMR-0072067.

[1] R. A. Guyer and P. A. Johnson, Phys. Today, No. 4, 30 (1999).
[2] R. A. Guyer, K. R. McCall, and G. N. Boitnott, Phys. Rev. Lett. **74**, 3491 (1995).
[3] D. J. Holcomb, J. Geophys. Res. **86**, 6235 (1981).
[4] T. B. Anderson, Nature (London) **202**, 272 (1964).
[5] F. A. Donath, Am. Geophys. Union Trans. **45**, 103 (1964).
[6] M. S. Paterson and L. E. Weiss, Nature (London) **195**, 1046 (1962).
[7] M. S. Paterson and L. E. Weiss, Geol. Soc. Am. Bull. **77**, 343 (1966).
[8] M. W. Barsoum, T. Zhen, S. R. Kalidindi, M. Radovic, and A. Murugaiah, Nat. Mater. **2**, 107 (2003).
[9] A. Murugaiah, M. W. Barsoum, S. Kalidindi, and T. Zhen, J. Mater. Res. **9**, 1139 (2004).
[10] M. W. Barsoum, A. Murugaiah, S. R. Kalidindi, T. Zhen, and Y. Gogotsi, Carbon **42**, 1435 (2004).
[11] F. C. Frank and A. N. Stroh, Proc. Phys. Soc. London **65**, 811 (1952).
[12] The propagation of an IKB is not unlike the unstable propagation of a crack in a brittle solid [11]. In Ref. [11] it was assumed that once an IKB reached a free surface it would dissociate into two parallel noninteracting walls. The idea that an IKB can reach a grain boundary and not dissociate was not considered; we had to invoke it to explain our recent results [8–10].
[13] J. S. Field and M. V. Swain, Carbon **34**, 1357 (1996).
[14] N. Iwashita, M. V. Swain, J. S. Field, N. Ohta, and S. Bitoh, Carbon **39**, 1525 (2001).
[15] L. E. McNeil and M. Grimsditch, J. Phys. Condens. Matter **5**, 1681 (1993).
[16] T. Zhen, Ph.D. thesis, Drexel University, Philadelphia, PA, 2004.
[17] A. Meike, Am. Mineral. **74**, 780 (1989).
[18] A. Kronenberg, S. Kirby, and J. Pinkston, J. Geophys. Res. **95**, 19 257 (1990).
[19] I. A. Bell and C. J. Wilson, Tectophysics **78**, 201 (1981).
[20] M. W. Barsoum and T. El-Raghy, Met. Mater. Trans. A **30**, 363 (1999).
[21] M. W. Barsoum, L. Farber, T. El-Raghy, and I. Levin, Met. Mater. Trans. A **30**, 1727 (1999).
[22] L. Farber, I. Levin, and M. W. Barsoum, Philos. Mag. Lett. **79**, 163 (1999).
[23] M. W. Barsoum, Prog. Solid State Chem. **28**, 201 (2000).
[24] M. W. Barsoum, D. Brodkin, and T. El-Raghy, Scr. Metall. Mater. **36**, 535 (1997).
[25] C. J. Gilbert, D. R. Bloyer, M. W. Barsoum, T. El-Raghy, A. P. Tomsia, and R. O. Ritchie, Scr. Mater. **42**, 761 (2000).
[26] M. W. Barsoum and T. El-Raghy, J. Mater. Synth. Process. **5**, 197 (1997).
[27] A. N. Stroh, Proc. R. Soc. London A **223**, 404 (1954).
[28] R. Christoffersen and A. K. Kronenberg, J. Struct. Geol. **15**, 1077 (1993).
[29] B. Capogrosso-Sansone, Phys. Rev. B **66**, 224101 (2002).
[30] P. P. Delsanto and M. Scalerandi, Phys. Rev. B **68**, 064107 (2003).
[31] A. Moussatov and V. Gusev, Phys. Rev. Lett. **90**, 124301 (2003).
[32] M. W. Barsoum, M. Radovic, P. Finkel, and T. El-Raghy, Appl. Phys. Lett. **79**, 479 (2001).